

# Modeling Virion Growth in the Context of a Lytic Pathway

Cecile Dinh, Leon Garcia, Ivan Grubisic and Marwan Mustafa

May 12, 2009

# Contents

<b>1</b>	<b>Introduction</b>	<b>3</b>
1.1	Virion Growth . . . . .	3
1.2	Reaction Kinetics . . . . .	4
<b>2</b>	<b>Virion Production</b>	<b>4</b>
2.1	Description of the Model . . . . .	4
2.2	Deriving the Differential Equations . . . . .	5
2.3	Deterministic Solution . . . . .	6
2.4	Stochastic Solution . . . . .	6
2.4.1	Monte Carlo Simulations . . . . .	6
2.4.2	Monte Carlo in Virion Lattices . . . . .	7
<b>3</b>	<b>Lytic Pathway</b>	<b>9</b>
3.1	Description of the Model . . . . .	9
3.2	Deriving the Differential Equations . . . . .	10
3.3	Equilibrium Analysis . . . . .	11
3.4	Bifurcation Analysis of $a_{crit}$ . . . . .	13
<b>4</b>	<b>Discussion</b>	<b>14</b>
4.1	Potential Improvements . . . . .	14
4.2	Conclusion . . . . .	15

# 1 Introduction

## 1.1 Virion Growth

Virology is an important subject that can lead to the prevention, treatment, and eradication of various diseases. The manner in which a virus can infect a cell has been widely researched and analyzed. Most models concerning the rate of cell infection, however, focus on the ratio of uninfected cells to the concentration of virions present. Yet other factors, such as the replication rate of DNA within a cell, must also be taken into account.

The basic unit of a virus, known as a virion, consists of a capsule made of protein (a capsid) that encloses the virion genome, which can either be DNA or RNA (Figure 1). Sometimes the virion may have an envelope as well, consisting of a phospholipid bilayer not unlike that of a cell. A viral infection may take one of two pathways, lytic or lysogenic, or a combination of both. Through the lytic pathway, the virion injects its genome into a cell. The cell's machinery then creates viral components, which are then assembled within the cell to create virions. Once the virions fill the cell to capacity, the cell bursts, releasing many virions to continue infecting other cells. In the lysogenic pathway, the virion's nucleic acid is inserted directly into host the cell's DNA genome. Thus, when the cell replicates itself, the virion's genome is replicated as well [4]. The transition between the two pathways is dependent on "switch like" processes within the cell and will not be discussed in this study.

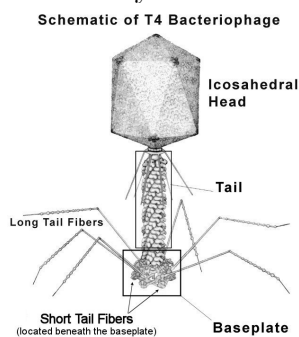


Figure 1: A schematic of the Bacteriophage capsid as rendered by Petr Leiman (Purdue Univ.)

In this paper, we first attempt to recreate Zhdanov's work in "Stochastic kinetics of reproduction of virions inside a cell" (2004). Using Monte Carlo (MC) simulations, we generically model and explain the growth of virion capsids within a single cell. Then, by applying chemical reaction kinetics to our system, we model the rates at which the virions are replicating with respect to genome replication, as well as mRNA and protein degradation. We examine how assuming a steady-state approximation can help yield the rate of virion release from a cell. These models can be helpful in determining the

rates of infection within organisms, which will aid in understanding virion dynamics so that new pharmaceuticals may better target virus replication lifecycles.

## 1.2 Reaction Kinetics

Reaction kinetics are used to explain the speed with which a chemical reaction can occur as influenced by a variety of environmental factors. Generally speaking, reaction kinetics deals with the combination of two reactants to form a product. In many cases, this is often simplified to general reaction schemes like in (1). In higher level systems, the interactions between substrates and enzymes have been described through the use of Michaelis-Menten equations, in which the initial reaction rate and the substrate concentration are related to one another [7].



It is important to keep in mind when considering these reaction kinetic rates, that mass is conserved, based on the laws of physics. Thus, the rates dictate the amount of reactants and products present at any point in time inside the system. The different reactions of the system can be combined to form an arrangement of differential equations, in which an essential assumption must be made: a steady-state approximation [12]. A system is considered to be in a steady state when the amounts of reactants and products remain constant over time despite factors that are designed to alter them. In order for a system to reach steady state, the rates of production and degradation must be the same. In a sense, this means that the population of a specific entity remains constant. The steady-state approximation, then, is an important tool, allowing for a reduction of the number of differential equations that need to be considered.

## 2 Virion Production

### 2.1 Description of the Model

When virions initially infect a cell, the virus takes over the cells own tools of replication and utilizes them to reproduce. The steps of reproduction are described in Figure 2. As the viral genome, either DNA or RNA, replicates, the process leads to the production of mRNA.

The mRNA codes for the proteins that will form an icosahedral structure around the viral genome called a capsid (see Figure 1). Once the capsids are released into the blood stream, they are referred to as virions, and these are the units that infect new cells.

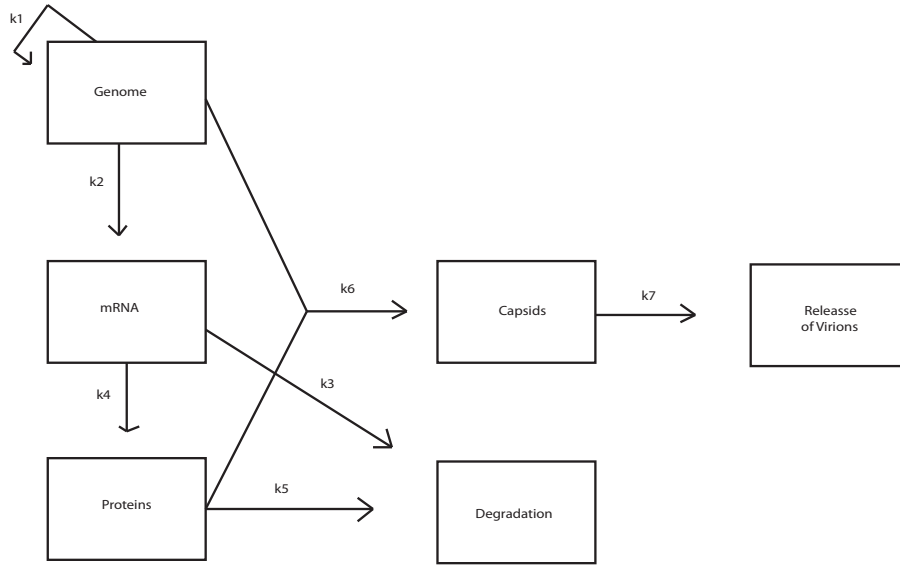


Figure 2: A flow diagram illustrating the mass action law that was used to derive the differential equations that govern the kinetics of virion growth within a cell.

## 2.2 Deriving the Differential Equations

Because the production of capsids puts the host cell machinery through added strain, processes like these lead to cell death. Our model will assume these processes to be harmless to the cell as far as cell machinery deterioration is concerned. The following equations are derived from Figure 2 and allow the virus-formation kinetics to be expressed in terms of the number of genomes,  $N_G$ , the number of mRNA copies,  $N_R$ , the number of proteins,  $N_P$ , and the number of capsids,  $N_V$ , within the cell by the application of the mass-action laws:

$$\dot{N}_G = k_1 N_G - k_6 N_P N_G \quad (2)$$

$$\dot{N}_R = k_2 N_G - k_3 N_R \quad (3)$$

$$\dot{N}_P = k_4 N_R - k_5 N_P - n k_6 N_P N_G \quad (4)$$

$$\dot{N}_V = k_6 N_P N_G - k_7 N_V \quad (5)$$

(2) describes the rate of change of the number of genomes, where  $k_1$  is the rate of genome replication and  $k_6$  is the rate of capsid formation as described by the joint states of  $N_G$  and  $N_P$ . Transcription increases the amount of mRNA at a rate of  $k_2$  and is then degraded at a rate of  $k_3$ , as shown by (4). The translation of proteins, described in (4) by  $k_4$ , does not directly affect the quantity of mRNA and therefore is not considered in (3). (5) shows that the number of capsids increases with a rate  $k_6$ , and are released from the cell at a rate of  $k_7$ . When considering these equations, it is important to keep in mind the condition  $\frac{N_P}{v} < c$ . This condition represents the critical

concentration of capsids inside the cell and means that the cell is saturated with capsid proteins.

As mentioned previously, the steady state approximation is the first simplification that will be applied to the system of equations. Under such considerations, mRNA and protein synthesis and degradation are both very quick processes in regards to the relative time scale and it is therefore appropriate to assume that both  $\frac{dN_R}{dt} = 0$  and  $\frac{dN_P}{dt} = 0$ . During steady state, the rate of virion production inside the cell,  $k_6$ , goes to zero, as the critical concentration within the cell is reached, leading to a further simplification.

$$N_R = \frac{k_2}{k_3} N_G \quad (6)$$

$$N_P = \frac{k_4 k_2}{k_3 k_5} N_G \quad (7)$$

The approximation reduces the problem from a system of four equations to only two equations. (8) and (9) represent the new system of equations and they introduce a new rate constant,  $k_0$ , which is equivalent to  $\frac{k_2 k_4 k_6}{k_3 k_5}$ .

$$\frac{dN_G}{dt} = k_1 N_G - k_0 N_G^2 \quad (8)$$

$$\frac{dN_V}{dt} = k_0 N_G^2 - k_7 N_V \quad (9)$$

Solving the new system of equations gives the following solutions for  $t \gg 0$ .

$$N_G^{ss} = \frac{k_1}{k_0} \quad (10)$$

$$N_V^{ss} = \frac{k_0}{k_7} N_G^2 \quad (11)$$

## 2.3 Deterministic Solution

The genome and virion population results were then plotted in Figure 3. This is an exact replication of the deterministic results from Zhdanov's paper.

## 2.4 Stochastic Solution

### 2.4.1 Monte Carlo Simulations

Monte Carlo simulations are capable of providing approximate solutions to large scale problems. They have often been used in molecular dynamics simulations to determine

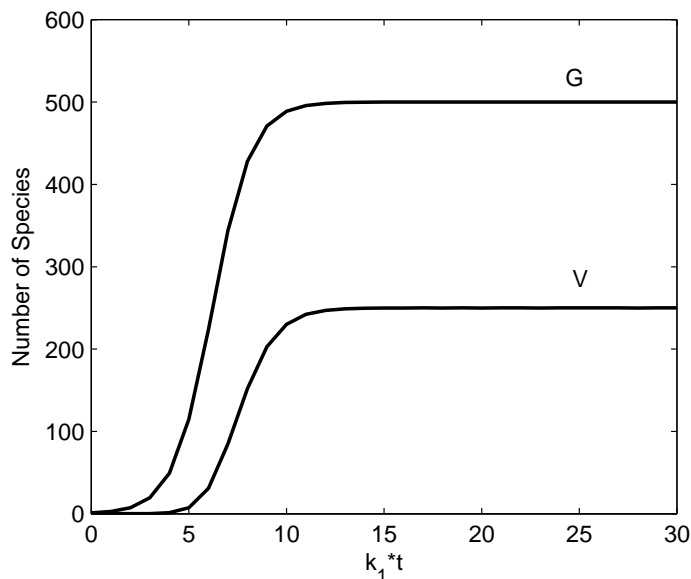


Figure 3: The deterministic solution of the system of equations provided by (8)-(9) using the MATLAB function *ode45*. The ratios  $\frac{k_0}{k_1} = 0.002$  and  $\frac{k_7}{k_1} = 2$  were used to determine the rate constants  $k_1$ ,  $k_0$  and  $k_7$ .

how a protein may move from one conformational state to another [17]. MC functions by locating sites at random within a system and either filling or vacating the site, depending on the current state of that site and the corresponding factors that affect it. The simulation is carried out until the system reaches equilibrium, making it an accurate method by which the dynamics of a system can be studied. MC simulations have one large drawback though; they are time consuming [14]. MC is therefore best used in either simple cases for long time scales, or large systems with short time scales.

#### 2.4.2 Monte Carlo in Virion Lattices

In the case of virion growth, Zhdanov used a Monte Carlo simulation to attain a steady state solution for the assembly of proteins on a single capsid. Remembering back to Figure 1 shows that the proteins of the capsid are assembled in an icosahedral structure. The lattice of triangles, shown in Figure 4 is a 2D layout of the expected 3D icosahedral structure. Each site is defined by  $\mu$ , the chemical potential, and  $E_0$ , the energy shift caused by the potential for neighbor interactions. The overall energy of the system will be determined by looking at the number of neighbors present within the same triangle,  $l$ , and the number of neighbors in the neighboring triangles,  $m$ . This is visually described in Figure 4. The maximum values of  $l$  and  $m$  are two and four respectively. Figure 4 shows an image of a 6 by 6 lattice as an example. The actual simulation will be done

on a 12 by 12 lattice.

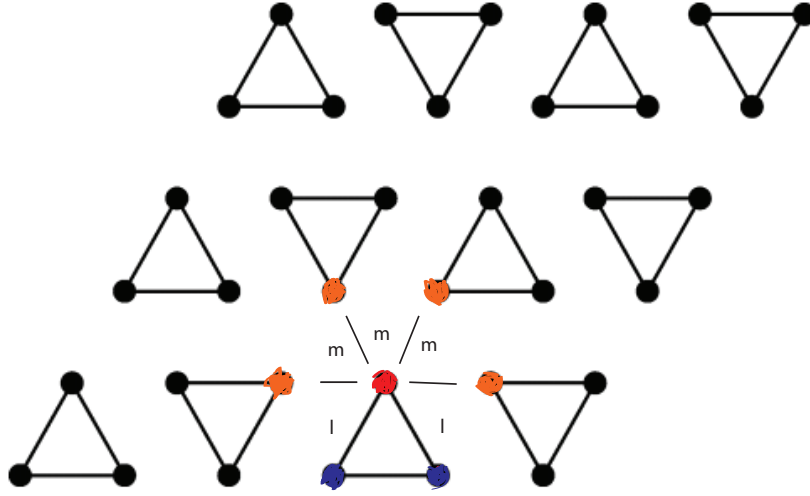


Figure 4: A 6x6 lattice which illustrates the manner in which the proteins of the capsid are assembled. The red dot is the site of interest. The orange dots are the four neighbors for nearby triangles that are described by  $m$ . The two blue dots are the neighbors within the same triangle that are described by  $l$  (A modified version of Figure 1 from [20]).

Since Monte Carlo simulations randomly identify sites within the lattice, there needs to be a consideration about the likelihood of either populating or depopulating a state. If the site is initially empty, then  $\rho$ , a random number from 0 to 1, represents the free energy the site can withstand. On the other hand if the site is filled,  $\rho$  is a measure of how many neighbors the protein is interacting with. If a site is vacant it will be populated when  $e^{\frac{\mu+E_0}{k_b*T}}$  is greater than  $\rho$ , where  $E_0$  is the initial energy and equivalent to  $\epsilon_1+2\epsilon_2$ . As the system becomes populated the energy will increase to  $E_1 = l*\epsilon_1+m*\epsilon_2$  for  $0 \leq l \leq 2$  and  $0 \leq m \leq 4$ . Conversely vacating a populated state is when  $e^{\frac{E_1}{k_b*T}}$  will occur greater than  $\rho$ .

A new random number  $\rho$  is assigned for each MC of the 10,000 steps that the simulation is run for. Another point of clarification for the MC is that phrase free energy means the total amount of energy that the site can handle. If the energy of inserting a protein at an empty site is less than the free energy (i.e. greater than  $\rho$ ), then the protein can fill the site. In the case of the filled site, the neighbor interactions, quantified by  $l$  and  $m$ , provide the framework in the 3D space for the capsid to remain intact. If a site has been occupied, but has no neighbors to bind with, then it is possible to imagine the protein moving through space and not remaining in that site. Therefore in this instance,  $\rho$  is the minimum number of neighbor interactions needed to keep the site populated. This means that if  $e^{\frac{E_1}{k_b*T}}$ , where we remember  $E_1$  depends on the neighbor interactions,

is less than  $\rho$  (i.e. greater than the minimum number of neighbor interactions), the site will remain populated.

Figure 5 shows that it is possible for the proper chemical potential,  $\mu$ , to achieve a steady state where all of the sites are occupied by a protein. This would then be the situation when a successfully assembled capsid exists. If it is possible to stochastically model the assembly of a single capsid, then it should also be possible to stochastically simulate the entire model.

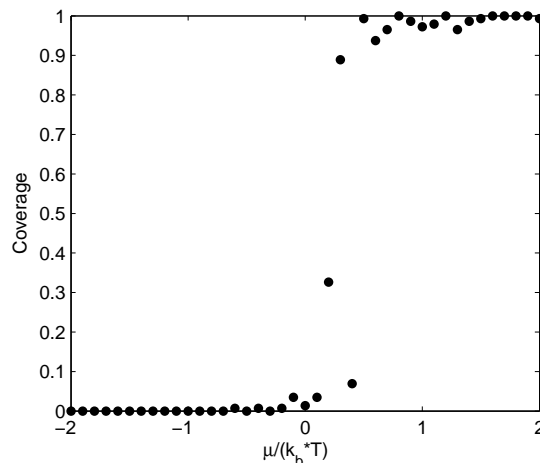


Figure 5: Protein coverage of a 144 site protein lattice (i.e. a  $12 \times 12$  triangular lattice), where the coverage depends on the chemical potential  $\frac{\mu}{k_b * T}$  for  $\frac{\epsilon_1}{k_b * T} = -2$  and  $\frac{\epsilon_2}{k_b * T} = -0.5$ . The figure was rendered in MATLAB 2009a.

## 3 Lytic Pathway

### 3.1 Description of the Model

The presence of virions in the blood stream will lead to an immune response from the body which will then work to decrease the number of infected cells, at a rate  $\delta$ , and free virions, at a rate  $\gamma$ . Figure 6 shows the flow diagram used to derive the differential equations governing a pseudo lytic pathway. It is pseudo lytic because, unlike in normal lytic pathways, the initially infected cell does not burst and cause a decrease to the total number of cells in the system. Because the total number of cells in the system is on the order of  $10^{10}$ , and deviations caused by the bursting of individual cells will not create noticeable changes. For the same reason, this model does not take into account the birth or death of cells.

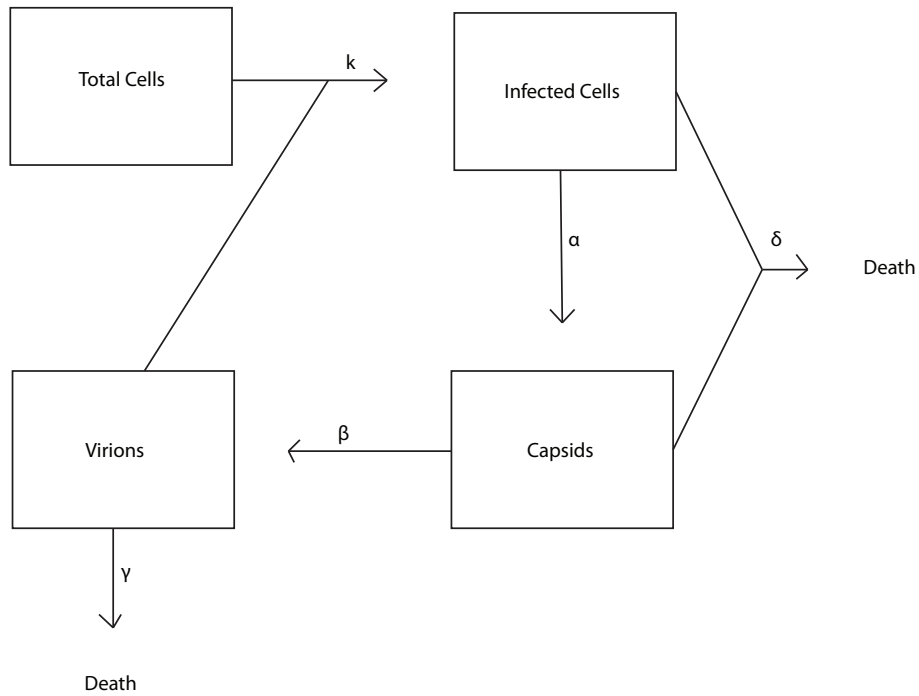


Figure 6: Flow diagram used to derive the differential equations that govern the kinetics of a lytic pathway in a culture of healthy cells.

The production of capsids described in Figure 2 is conglomerated into a single step with rate  $\alpha$  in Figure 6. Virions,  $V$ , infect healthy cells at a rate  $k$ ; healthy cells are defined as the total number of cells minus the infected cells (i.e.  $T-I$ ). More capsids,  $D$ , are produced, leading to their subsequent release at rate  $\beta$ . This model was described by [8].

### 3.2 Deriving the Differential Equations

The following differential equations are derived from Figure 6:

$$\dot{I} = kV(T - I) - \delta I \quad (12)$$

$$\dot{D} = \alpha I - \beta D - \delta D \quad (13)$$

$$\dot{V} = \beta D - \gamma V \quad (14)$$

Depending on the virus, the rate constants for the above equations will cover a range of orders of magnitude. Non-dimensionalizing the system of equations will allow for a clear analysis regardless of which virus is being considered. The first step is to normalize the number of cells, dividing the infected cells, capsids and virions by the total number of cells present.

$$\left\{ \begin{array}{l} i = \frac{I}{T} \\ d = \frac{D}{T} \\ v = \frac{V}{T} \end{array} \right.$$

The next step is to address the parameters and to determine which ones depend on one another. The ability of a virion to infect a healthy cell is a process that is independent of all the other rates and can be left alone. The rates of capsid production and release,  $\alpha$  and  $\beta$  respectively, are not independent, however. In lytic pathways, it is necessary to achieve a critical concentration of capsids within the cell for the cell's plasma membrane to break apart, releasing the capsids as virions into the blood stream. The relationship between these two processes can be represented as a ratio of the two rates. By looking through the data for a number of different viruses, this ratio was calculated to be  $\frac{\alpha}{\beta} = 0.02$ . A similar relationship can be established with the immune system's response to a virus. The immune response will be constant for the same threat, but its ability to clear the infection depends on its ability to reach the infection. Therefore, it would be reasonable to conclude that virions in the blood stream are cleared at a faster rate than infected cells within a tissue. This ratio was determined by looking at the clearance rates of Hepatitis B [8], giving:  $\frac{\gamma}{\delta} = 100$ . The dimensionless time scale is given by  $\tau = t * \delta$ . Final compilation of all dimensionless parameters is described by the following:

$$\left\{ \begin{array}{l} a = \frac{kT}{\delta} \\ b = \frac{\beta}{\delta} \end{array} \right.$$

Applying these changes leads to the following dimensionless system of differential equations where ' denotes differentiation with respect to  $\tau$ .

$$i' = av(1 - i) - i \quad (15)$$

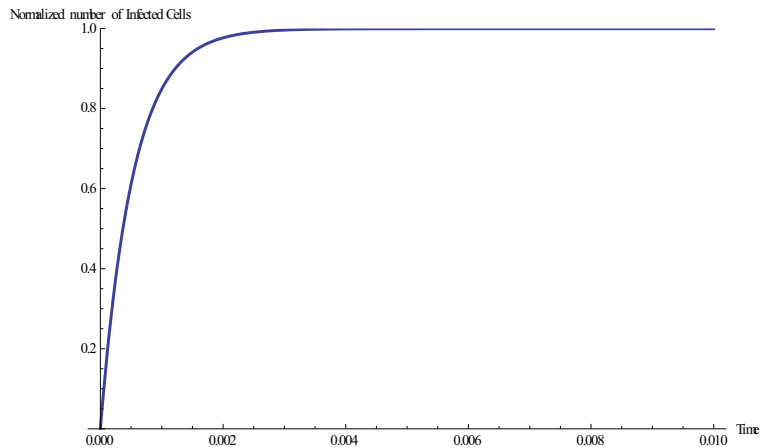
$$d' = 50bi - bd - d \quad (16)$$

$$v' = bd - 100v \quad (17)$$

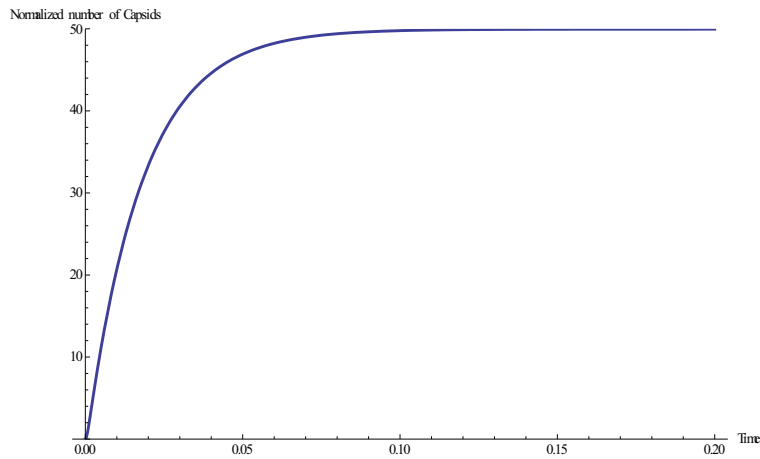
Analysis of the above systems reveals that the number of infected cells,  $i$ , reaches steady state much faster than  $d$  or  $v$  (Figure 7).  $i$  reaches its steady state in 0.002 time steps, while  $d$  reaches its in 0.05 time steps. It is therefore appropriate to assume  $i$  to be constant, further simplifying the system to two equations.

### 3.3 Equilibrium Analysis

The first step of analyzing the equilibrium point of (15)-(17) is linearizing the equations. Equilibrium analysis will be done for the system of three equations. While the



(a)



(b)

Figure 7: The steady state solutions for (15)-(16). This plot was made with Mathematica 7. (a) The number of infected cells. (b) The number of capsids.

system of two equations brings simplicity in arriving at a numerical solution, equilibrium analysis requires the use of all three equations due to its mathematically fragile nature. Computing the Jacobian matrix gives:

$$J(x, y, z) = \begin{pmatrix} -az - 1 & 0 & a - ax \\ 50b & -b - 1 & 0 \\ 0 & b & -100 \end{pmatrix} \quad (18)$$

From the Jacobian, it is possible to derive the characteristic polynomial, described by (19), at the equilibrium point (0,0,0).

$$p(\lambda) = -100 - b + 50ab^2 - 201\lambda - 101b\lambda - 102\lambda^2 - b\lambda^2 - \lambda^3 \quad (19)$$

To be able to understand the properties of the equilibrium point (0,0,0), we must first

understand the nature of the roots from (19). Since the characteristic polynomial is a negative cubic function, we can look at the critical points of  $p(\lambda)$ .

$$p'(\lambda) = -201 - 101b - 204\lambda - 2b\lambda - 3\lambda^2 \quad (20)$$

The critical points of this equation are  $t_{1,2} = \frac{1}{3}(-102 - b \pm \sqrt{9801 - 99b + b^2})$ . To guarantee that we have three real roots, and therefore three real eigenvalues at  $J(0,0,0)$ , we require the minimum to be negative and the maximum to be positive. Evaluating, it can be shown that the maximum value is always positive, while the minimum value is negative if and only if  $a$  satisfies

$$a < \frac{2b^3 + 19602(99 + SQRT) + b^2(-297 + 2SQRT) - 99b(297 + 2SQRT)}{1350b^2} \quad (21)$$

where  $SQRT = \sqrt{9801 - 99b + b^2}$ .

Since we also know that  $p(0) = -100 - 100b + 50ab^2$ , it is possible to determine the sign of the eigenvalues, leading to the following conditions.

1. All of the eigenvalues are negative if and only if  $a > 2\frac{(b+1)}{b^2}$
2. One eigenvalue is positive if and only if  $a < 2\frac{(b+1)}{b^2}$

From a biologically relevant stand point the second condition implies that we will have one nodal sink at  $(\frac{50(-2-2b+ab^2)}{ab(1+b)}, \frac{-2-2b+ab^2}{2a(1+b)})$  and one saddle point at  $(0,0)$ , whereas for the first condition there will be only a single nodal sink at  $(0,0)$ . Taking into account the original data from [8], Figure 8(a) shows the first condition where the virions and capsids will both crash to zero. Figure 8(b), on the other hand, shows the balanced system where there is a stable nodal sink at values  $d, v > 0$  and all of the susceptible cells in the system end up infected.

### 3.4 Bifurcation Analysis of $a_{crit}$

The bifurcation point described in the previous section is a transcritical point. This means that a stable point moves to being unstable, which is seen at the point  $(0,0)$  in the 2D system of  $v$  and  $d$  from Figure 8 when it changes from a nodal sink to a saddle point. A closer analysis of  $a_{crit} = 2\frac{(b+1)}{b^2}$  in terms of the order of magnitude for the parameters leads to a linear equation that reveals which parameters have the greatest effect upon to the system. Let  $\mathbf{j}$ ,  $\mathbf{k}$ ,  $\mathbf{m}$  and  $\mathbf{n}$  be the orders of magnitude for the following.

$\mathbf{j}$  The total number of susceptible cells

$\mathbf{k}$  The immune response

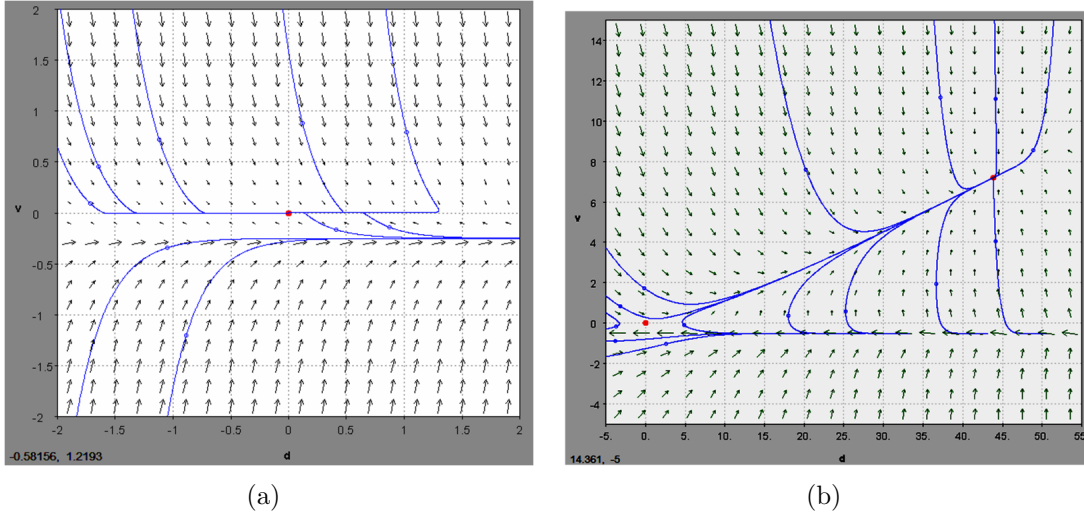


Figure 8: PPLANE phase diagrams of (16)-(17) for both sides of the bifurcation point. (a)  $a > 2\frac{(b+1)}{b^2}$  (b)  $a < 2\frac{(b+1)}{b^2}$ . The values for parameters  $a$  and  $b$  were taken from [8] and are for Hepatitis B

**m** The rate of capsid production/release

**n** The rate of infection of healthy cells

Implementing these into  $a_{crit}$  gives:

$$j = 5k - 3m - n \quad (22)$$

(22) gives us a coded response for the total number of cells needed for a virus to be able to sustain itself in culture. It implies that if the immune response were to increase by a single order of magnitude, the total number of cells in the system would have to increase by 5 orders of magnitude. This is a logical conclusion because if the infection is being cleared quicker than the cells can replicate and release capsids into the plasma, then the virus should die out. In those instances, we are at a position where  $a > a_{crit}$  and a single node exists at  $(0,0,0)$ . Figure 9 shows exactly how the system can either decrease to zero or reach a positive steady state.

## 4 Discussion

### 4.1 Potential Improvements

Being able to solve a model both deterministically and stochastically speaks to the robustness of the model. When a stochastic solution cannot be found, it is interesting

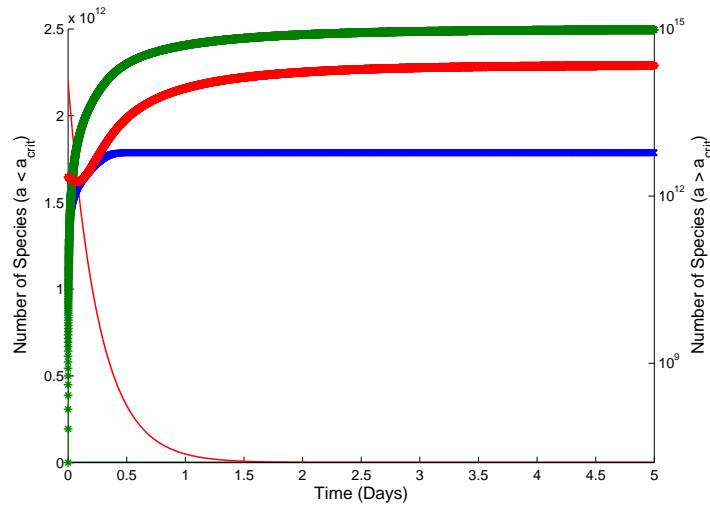


Figure 9: The number of species of I (blue), D (green) and V (red). The thicker lines are associated with  $a > a_{crit}$ . The initial conditions for the plot were  $I(0) = 0$ ,  $D(0) = 0$  and  $V(0) = 1000$ . The plot was generated using MATLAB 2009a.

to apply a "white noise" term,  $\epsilon * \sqrt{t} * norm(0,1)$ , where  $t$  is the time step and  $norm(0,1)$  is a independently distributed random number from 0 to 1. By varying the magnitude of  $\epsilon$ , it is possible to see what the size of the perturbations would have to be to disrupt the dynamics of the model. This would be applicable to both models discussed in this paper.

The initial Monte Carlo simulation that was done to determine whether or not it is possible to use a stochastic simulation with the virion growth model provided positive results. These results would seem to imply that a stochastic analysis of the entire model should be possible; however, there has been little success in our implementation of the Gillespie Algorithm [16]. We are unsure of where the exact error lies, but it would be of interest to implement this algorithm so as to have a full analysis of the virion growth model.

## 4.2 Conclusion

The most important result from this analysis is the relationship between the critical size of the culture and the three main parameters: immune response, capsid production and infection of susceptible cells. The relationship  $\mathbf{j} = 5\mathbf{k} - 3\mathbf{m} - \mathbf{n}$  gives important insight into the nature of viral growth. It implies that the most effective manner in combating the growth of a virus within the tissue is to increase the immune response at the site of the viral infection. From these results, it would be reasonable to promote the development of pharmaceutical drugs that allow the immune system to recognize the virus more efficiently. This will probably be the safest manner to combat the replication

of the virus. While affecting the production of new capsids within the cell is also an effective method to counter viral growth, this approach could have undesirable side-effects. It requires altering the signaling pathways in the nucleus that are responsible for either stimulating or suppressing transcription and subsequent translation in the cytoplasm. This could be a very risky procedure since these processes are necessary for the host cell's ability to perform its own functions. Subjecting healthy cells to such a treatment can easily lead to genomic mutations, impairing cell function and leaving the biological system more vulnerable to an infectious attack. Lastly, while targeting the ability of the virus to infect cells remains an option in combating viral growth, an efficient solution in this regard is beyond the capabilities of today's medicine. It would require the cell infection rate to be decreased by several orders of magnitude in order to have a favorable (i.e.  $a > a_{crit}$ ) impact against viral growth.

It is important to also keep in mind that the desired result is not always to kill off the virus. In research, it is often times required that a cell culture exist, either in vivo or in vitro, that can maintain a virus in stable conditions. Having the above relationship will allow researchers to create cell colonies of appropriate size, making better use of resources and time.

## References

- [1] BIASOLO, M. A., CALISTRI, A., CESARO, S., GENTILE, G., MENGOLI, C., AND PAL?, G. Case report: Kinetics of Epstein-Barr virus load in a bone marrow transplant patient with no sign of lymphoproliferative disease. *Journal of Medical Virology* 69, 2 (2003), 220–224.
- [2] BRACK, A. R., DIJKSTRA, J. M., GRANZOW, H., KLUPP, B. G., AND METTENLEITER, T. C. Inhibition of virion maturation by simultaneous deletion of glycoproteins e, i, and m of pseudorabies virus. *Journal of Virology* 73, 7 (July 1999), 53645372. PMC112592.
- [3] CASTIGLIONE, F., DUCA, K., JARRAH, A., LAUBENBACHER, R., HOCHBERG, D., AND THORLEY-LAWSON, D. Simulating Epstein-Barr virus infection with C-ImmSim. *Bioinformatics* 23, 11 (June 2007), 1371–1377.
- [4] FIELDS, B. N., KNIPE, D. M., HOWLEY, P. M., GRIFFIN, D. E., AND BERNARD N. FIELDS, D. M. K. *Fields' virology*. 2006.
- [5] GILLESPIE, D. T. Exact stochastic simulation of coupled chemical reactions. *The Journal of Physical Chemistry* 81, 25 (Dec. 1977), 2340–2361.
- [6] KLONOWSKI, W. Simplifying principles for chemical and enzyme reaction kinetics. *Biophysical Chemistry* 18, 2 (Sept. 1983), 73–87. PMID: 6626688.
- [7] MAROLEWSKI, A. Fundamentals of enzyme kinetics. revised edition by athel Cornish-Bowden. portland press, london. 1995. xiii + 343 pp. 17.5 cm 24.5 cm. ISBN 1-85578-072-0. \$29.00. *Journal of Medicinal Chemistry* 39, 4 (1996), 1010–1011.
- [8] MURRAY, J. M., PURCELL, R. H., AND WIELAND, S. F. The half-life of hepatitis b virions. *Hepatology* 44, 5 (2006), 1117–1121.
- [9] PERELSON, A. S., HERRMANN, E., MICOL, F., AND ZEUZEM, S. New kinetic models for the hepatitis c virus. *Hepatology* 42, 4 (2005), 749–754.
- [10] PERELSON, A. S., NEUMANN, A. U., MARKOWITZ, M., LEONARD, J. M., AND HO, D. D. HIV-1 dynamics in vivo: Virion clearance rate, infected cell Life-Span, and viral generation time. *Science* 271, 5255 (Mar. 1996), 1582–1586.
- [11] RAO, C. V., AND ARKIN, A. P. Stochastic chemical kinetics and the quasi-steady-state assumption: Application to the gillespie algorithm. *The Journal of Chemical Physics* 118, 11 (Mar. 2003), 4999–5010.
- [12] SCHNELL, S., AND MAINI, P. K. Enzyme kinetics at high enzyme concentration. b. math. *Biol* 62 (2000), 483499.

- 
- [13] SEGEL, L. On the validity of the steady state assumption of enzyme kinetics. *Bulletin of Mathematical Biology* 50, 6 (Nov. 1988), 579–593.
- [14] TAMA, F., AND BROOKS, I. I. I. C. L. SYMMETRY, FORM, AND SHAPE: guiding principles for robustness in macromolecular machines. Annual Reviews of Biophysics, May 2006.
- [15] TWAROCK, R. A tiling approach to virus capsid assembly explaining a structural puzzle in virology. *Journal of Theoretical Biology* 226, 4 (Feb. 2004), 482, 477.
- [16] ULLAH, M., SCHMIDT, H., CHO, K., AND WOLKENHAUER, O. Deterministic modelling and stochastic simulation of biochemical pathways using MATLAB. *Systems Biology, IEE Proceedings* 153, 2 (2006), 53–60.
- [17] VAN GUNSTEREN, W. F., AND BERENDSEN, H. J. C. Computer simulation of molecular dynamics: Methodology, applications, and perspectives in chemistry. *Angewandte Chemie International Edition in English* 29, 9 (1990), 992–1023.
- [18] ZHDANOV, V. Kinetic model of HIV infection. *Journal of Experimental and Theoretical Physics* 105, 4 (Oct. 2007), 856–860.
- [19] ZHDANOV, V. P. Bifurcation in a generic model of intracellular viral kinetics. *Journal of Physics A: Mathematical and General* 37, 5 (2004), L63–L66.
- [20] ZHDANOV, V. P. Stochastic kinetics of reproduction of virions inside a cell. *Biosystems* 77, 1-3 (Nov. 2004), 143–150.
- [21] ZHDANOV, V. P. Monte carlo simulation of bifurcation in the intracellular viral kinetics. *Physical Biology* 2, 1 (2005), 46–50.
- [22] ZHDANOV, V. P. Kinetic oscillations in the expression of messenger RNA, regulatory protein, and nonprotein coding RNA. *Chemical Physics Letters* 458, 4-6 (June 2008), 359–362.